

Machinability investigation and sustainability assessment in FDHT with coated ceramic tool

Asutosh Panda, Sudhansu Ranjan Das* and Debabrata Dhupal

Department of Production Engineering, Veer Surendra Sai University of Technology, Burla 768018, India

(Received May 217, 2019, Revised January 13, 2020, Accepted January 27, 2020)

Abstract. The paper addresses contribution to the modeling and optimization of major machinability parameters (cutting force, surface roughness, and tool wear) in finish dry hard turning (FDHT) for machinability evaluation of hardened AISI grade die steel D₃ with PVD-TiN coated (Al₂O₃-TiCN) mixed ceramic tool insert. The turning trials are performed based on Taguchi's L₁₈ orthogonal array design of experiments for the development of regression model as well as adequate model prediction by considering tool approach angle, nose radius, cutting speed, feed rate, and depth of cut as major machining parameters. The models or correlations are developed by employing multiple regression analysis (MRA). In addition, statistical technique (response surface methodology) followed by computational approaches (genetic algorithm and particle swarm optimization) have been employed for multiple response optimization. Thereafter, the effectiveness of proposed three (RSM, GA, PSO) optimization techniques are evaluated by confirmation test and subsequently the best optimization results have been used for estimation of energy consumption which includes savings of carbon footprint towards green machining and for tool life estimation followed by cost analysis to justify the economic feasibility of PVD-TiN coated Al₂O₃+TiCN mixed ceramic tool in FDHT operation. Finally, estimation of energy savings, economic analysis, and sustainability assessment are performed by employing carbon footprint analysis, Gilbert approach, and Pugh matrix, respectively. Novelty aspects, the present work: (i) contributes to practical industrial application of finish hard turning for the shaft and die makers to select the optimum cutting conditions in a range of hardness of 45-60 HRC, (ii) demonstrates the replacement of expensive, time-consuming conventional cylindrical grinding process and proposes the alternative of costlier CBN tool by utilizing ceramic tool in hard turning processes considering technological, economical and ecological aspects, which are helpful and efficient from industrial point of view, (iii) provides environment friendliness, cleaner production for machining of hardened steels, (iv) helps to improve the desirable machinability characteristics, and (v) serves as a knowledge for the development of a common language for sustainable manufacturing in both research field and industrial practice.

Keywords: machinability; hard turning; AISI D3 steel; optimization; economical analysis; sustainability assessment

1. Introduction

Nowadays, hardened steel materials ranging from 42-68 HRC have great demand for manufacturing of precision components to attain high mechanical performance in different engineering applications. Moreover, these materials are extensively used for manufacturing of automotive parts, bearings, dies and moulds, and machine tool components requiring specific characteristics (excellent indentation resistance, relatively low ductility, high value of hardness-to-elastic modulus ratio, and superior abrasiveness), which makes hard-to-machine (Astakhov 2008, Suresh *et al.* 2013) Traditionally, the most common method for machining the hardened steels is associated with a long technological chain of time-consuming and expensive operations, as illustrated in Figure 1a. In recent past, hard turning has become a well-developed innovative machining approach that offers potential benefits over conventional cylindrical grinding that includes; (i) excellent

process flexibility, (ii) faster manufacturing cycle times, (iii) reduced setup times, (iv) eco-friendly production without use of hazardous cutting fluid, (v) higher material removal rate, and (vi) considerable savings in carbon footprints via. reduced energy consumption (Grzesik 2008, Anand *et al.* 2019) (refer, Fig. 1(b)).

Since, hardened steel materials are extremely difficult-to-cut, machinability improvement is of prime importance, which is a challenging task due to the following critical issues; excessive tool wear, high heat generation, higher power consumption, large cutting force, and undesirable surface quality with difficulty in chip carrying management. Consequently, due to complex-dynamic behavior of hard turning process and its close connection with various parameters, the achievement of high responsiveness of production is very essential from techno-economical and ecological aspects. Moreover, for successful implementation of hard turning technology in substitute of traditional cylindrical grinding in machining of different hardened steels can be improved in terms of cutting efficiency, quality, cost, and productivity by considering the most appropriate and optimal process parameters. Under such circumstances, the effective utilization of

*Corresponding author, Dr.
E-mail: das.sudhansu83@gmail.com

experimental, modeling, and optimization methodology make possible a greater improvement in decision-making with new technological solution that can simultaneously satisfy and control the several distinctive as well as contradictory objectives (multi-response) in order to make the hard turning process as an excellent choice for machining of hardened steel materials. Several statistical and computational approaches such as MRA (Bartarya *et al.* 2013, Bensouilah *et al.* 2016, Khellaf *et al.* 2016), RSM (Hessainia *et al.* 2013; Tang *et al.* 2014, Bouzid *et al.* 2014, Fnides *et al.* 2015), ANN (Quiza *et al.* 2008, Gaitonde *et al.* 2010, Asiltürk 2012, Nouioua *et al.* 2017, Zerti *et al.* 2018) have been applied for predictive modelling and Taguchi method (Günay and Yücel 2013, Xiao *et al.* 2016, Zerti *et al.* 2016), GRA (Sahoo and Sahoo 2013, Bouacha *et al.* 2014, Panda *et al.* 2016), desirability function approach of RSM (Meddour *et al.* 2014, Shihab *et al.* 2014, Sanjeev Kumar *et al.* 2016, Benlahmidi *et al.* 2016), GA (Laouissi *et al.* 2018; Meddour *et al.* 2018, Das *et al.* 2018), PSO (Bouacha and Terrab 2016, Panda *et al.* 2017, Xie *et al.* 2018) have been employed for parametric as well as process optimization in hard turning. Extensive studies have been reported by employing various experimental designs, modelling techniques and optimization approaches in order to assess or investigate the machinability (Davim and Figueira *et al.* 2007, Gaitonde *et al.* 2009a, Suresh *et al.* 2012, Chinchankar *et al.* 2013, Aouici *et al.* 2014, Nayak and Sehgal 2015, Das *et al.* 2015, Kumar and Chauhan, 2015, Das *et al.*, 2016; Mondal and Das, 2017; Ramanuj Kumar *et al.* 2018), to predict the various machinability parameters, and to control the process parameters in finish dry hard turning of different workpiece materials (42CrMo4, X210Cr12, EN-24, EN-32, AISI 1045, 1040, 420, 4340, 4140, 52100, D2, D3, D6, H11).

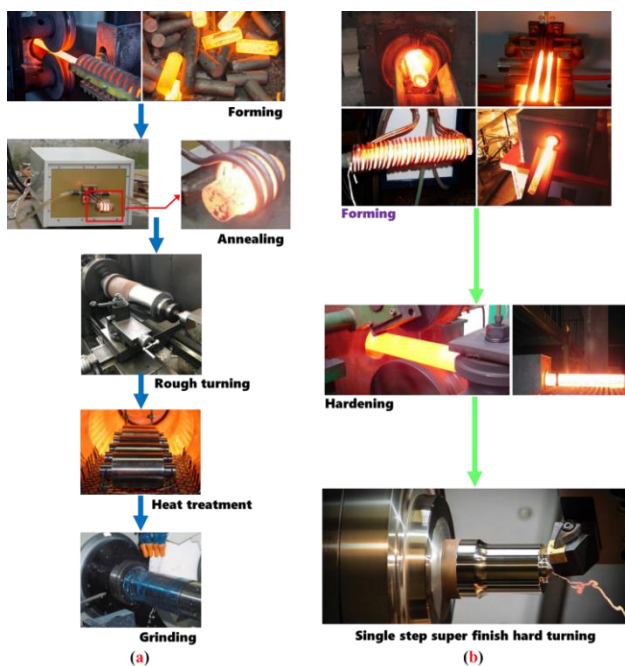


Fig. 1 (a) Technological series of traditional manufacturing processes, and (b) hard turning production

As par with existing literature till due, systematic analysis on machinability under dry cutting environment is quite inadequate. In particular, very limited research works have been reported concerning FDHT of AISI D₃ steel. Comparatively, now yet almost no investigator has conducted experiment analysis combining both the geometrical and cutting parameters while hard turning of AISI D₃ steel using PVD-TiN coated Al₂O₃+TiCN mixed ceramic tool. The literature divulges a series of published research applying any one technique (statistical or computational) rather than considering both techniques to solve multi-response problem, which plays a very important role for enhancement of machining performance as well as improvement of machinability. Literature review highlights that the realistic approach to justify the use of PVD-TiN coated Al₂O₃+TiCN mixed ceramic tool as profitably substituting costly CBN and PCBN tool materials in hard turning process is less outlined, which finds the scope for researchers. Moreover, the investigation deals with energy savings and sustainability assessment in hard turning typically, in today's manufacturing society that ensures green development towards safer environment is still unexplored, which finds an ideal worthy of investigation in the present paper. In view of such contribution, the current study aims to analyze the accomplishment of cutting performance for PVD-TiN coated Al₂O₃+TiCN mixed ceramic tool, and to investigate the machinability of hardened steel (AISI D₃ - 61HRC) concerning cutting force, tool wear, surface roughness, and chip morphology by considering geometrical parameters (approach angle, nose radius) and machining parameters (speed, feed rate, depth of cut). Taguchi's L₁₈ orthogonal array (OA), multiple regression analysis (MRA), and statistical technique (RSM) followed by computational approach (GA, PSO) are subsequently employed for experimental investigation, predictive modelling, and multi-response optimization. Subsequently, the best optimal solution is used respectively, for economic analysis and energy saving carbon footprint analysis in order to rationalize the usefulness of PVD-TiN coated Al₂O₃+TiCN mixed ceramic tool in hard turning applications, and the reduction in energy consumption as well as greenhouse gas emissions with an intension to raise the awareness of green manufacturing and clean production in the manufacturing industry. Lastly, the Pugh matrix environmental approach has been proposed for sustainability assessment of finish dry hard turning process. This experimental observation relates to process improvement in industrial applications quite helpful and efficient from economic point of view.

2. Experimental setup and procedure

In the present experimental investigation, high carbon-high chromium AISI D₃ steel of cylindrical bar having dimensions $\phi 45 \times 200$ mm (diameter and length, respectively) is considered as workpiece material due to excellent wear resistance and its widely application in mould and die making industries. Table 1 shows the chemical composition of AISI D₃ steel and confirms the

Table 1 Chemical composition of AISI D3 steel

Elements	C	Cr	Mn	Si	Ni	V	Mo	P	S	Fe
Weight percentage	1.973	11.463	0.354	0.32	0.265	0.047	0.02	0.016	0.009	Remainder

Table 2 Cutting and geometrical parameters associated with their levels

Parameters	Levels		
	1	2	3
Approach angle, K_r ($^\circ$)	75	95	-
Nose radius, r (mm)	0.4	0.8	1.2
Cutting speed, V (m/min)	110	180	250
Feed, f (mm/rev)	0.06	0.11	0.16
Depth of cut, a (mm)	0.1	0.2	0.3

Table 3 Experimental plan layout and results

Test no.	Coded values					Actual settings					Machinability parameters		
	K_r	r	V	f	a	K_r ($^\circ$)	r (mm)	V (m/min)	f (mm/rev)	a (mm)	Flank wear, VB (mm)	Cutting force, F_c (N)	Roughness, R_a (μm)
1	1	1	1	1	1	75	0.4	110	0.06	0.1	0.114	62.73	0.551
2	1	1	2	2	2	75	0.4	180	0.11	0.2	0.151	113.15	1.164
3	1	1	3	3	3	75	0.4	250	0.16	0.3	0.178	220.98	1.988
4	1	2	1	1	2	75	0.8	110	0.06	0.2	0.137	91.47	0.295
5	1	2	2	2	3	75	0.8	180	0.11	0.3	0.186	166.14	0.745
6	1	2	3	3	1	75	0.8	250	0.16	0.1	0.215	122.79	1.510
7	1	3	1	2	1	75	1.2	110	0.11	0.1	0.142	80.29	0.395
8	1	3	2	3	2	75	1.2	180	0.16	0.2	0.216	134.87	0.850
9	1	3	3	1	3	75	1.2	250	0.06	0.3	0.258	212.50	0.230
10	2	1	1	3	3	95	0.4	110	0.16	0.3	0.149	92.36	1.484
11	2	1	2	1	1	95	0.4	180	0.06	0.1	0.173	68.13	0.291
12	2	1	3	2	2	95	0.4	250	0.11	0.2	0.193	118.29	0.926
13	2	2	1	2	3	95	0.8	110	0.11	0.3	0.176	146.46	0.707
14	2	2	2	3	1	95	0.8	180	0.16	0.1	0.201	70.25	1.274
15	2	2	3	1	2	95	0.8	250	0.06	0.2	0.235	110.74	0.292
16	2	3	1	3	2	95	1.2	110	0.16	0.2	0.185	159.71	0.981
17	2	3	2	1	3	95	1.2	180	0.06	0.3	0.221	101.82	0.395
18	2	3	3	2	1	95	1.2	250	0.11	0.1	0.267	80.35	0.786

elemental composition of workpiece material after performing the test through stationary metal analyzer (SpectroMax). Prior to machining, (i) specimen materials were heat treated by quenching followed by tempering at 900°C and 420°C respectively, (ii) oxide layers were removed from the exterior surface, and (iii) specimens were mounted on tailstock. With the courtesy of the heat treatment process, there was an enhancement of hardness to 61 HRC due to formation of different microstructures (martensite and ferrite). Commercially available grade AB2010 (make: Taegutec) PVD-TiN coated Al_2O_3 -TiCN

mixed ceramic of coating layer thickness 1 μm (Fig. 2(a)) has been chosen as cutting tool. The elemental constituents and thickness of the coating were identified (refer, Fig. 2) in a scanning electron microscope (SEM) with an embedded energy dispersive X-ray (EDS) analyzer. Cutting inserts with three different nose radius (ISO designation: CNGA 120404, CNGA 1204108, CNGA 120412) are clamped rigidly on the ISO designated two different tool holders of PCBNL 2525M12 and PCLNL 2525M12 which resulted the following cutting geometry: clearance angle of 0 $^\circ$, approach angles of 75 $^\circ$ and 95 $^\circ$, back and side rake angle of -6 $^\circ$, point angle of 80 $^\circ$.

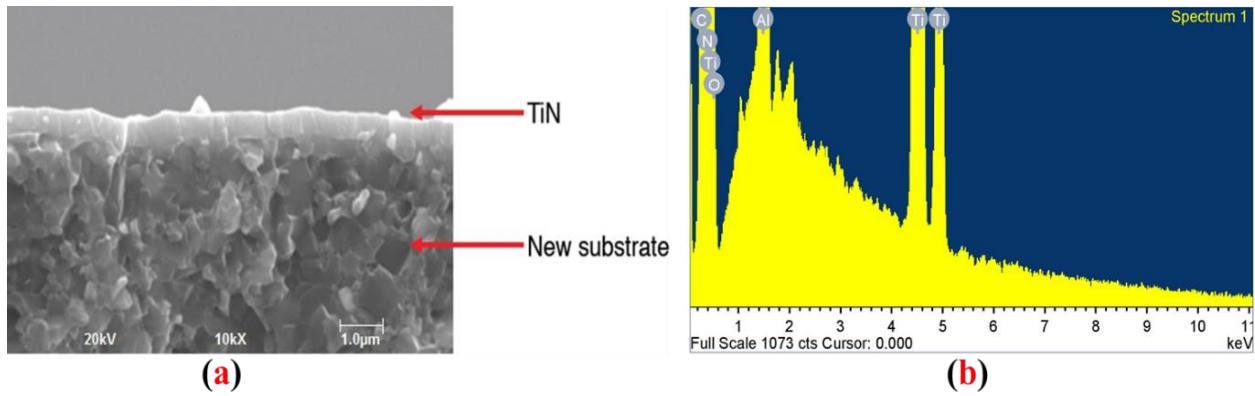


Fig. 2(a) SEM micrograph and (b) EDX analysis of coated layer

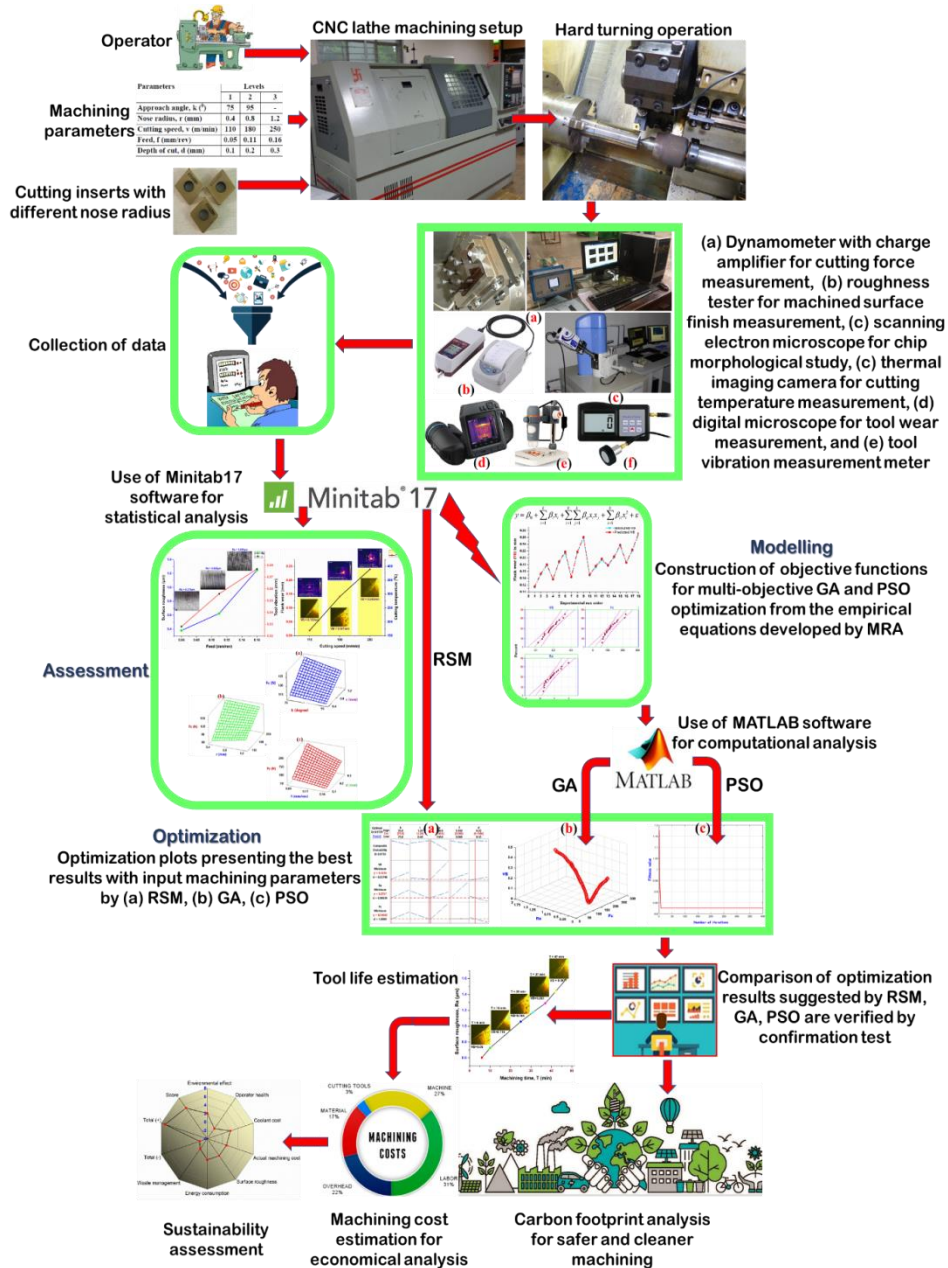


Fig. 3 Layout of experimental setup including methodology proposed

For performing the straight cylindrical turning under dry environment condition, a heavy-duty high accuracy CNC lathe (make: Batliboi, model: SPRINT 16TC) has been utilized with spindle power capacity and maximum spindle speed of 7.5 kW and 5000 rpm, respectively. During FDHT of AISI D3 steel, a piezoelectric dynamometer (make: Kistler, model: 9257B) is used to measure the principal cutting force (F_C). Measurement of surface finish of the machined part in terms of arithmetical mean roughness value (R_a) is measured with the help of SurfTest SJ-210 Mitutoyo roughness tester. After every successive experimental trial, the flank wear of the cutting tool is measured by using high resolution imaging digital microscope (make: Celestron, model: 44308-DS). For better understanding of hard turning process and machinability improvement, a comprehensive investigation is performed on work–tool interface temperature (cutting temperature), tool vibration, and morphological study of chips by employing thermal imaging camera (make: FLIR, model: T540) followed by digital vibration meter equipped with piezoelectric accelerometer (make: Mextech, model: VM6360), and last by scanning electron microscope (make: JEOL, model: JSM-6480LV). A simplified layout of the experimental setup including methodology proposed in this work, is presented in Fig. 3.

In this paper, five machining parameters (approach angle, machining speed, feed rate, depth of cut and, tool nose radius) and three major machinability parameters (surface roughness, cutting force and tool wear) are considered as input factors and output responses, respectively for machinability investigation, predictive modelling and process optimization. The selection of different levels of machining parameters are considered with reference to published research works and recommendation of cutting tool manufacturer. Table 2 illustrates the detailed input factors with their corresponding levels for the experiment in actual as well as coded values setting. The proposed experimental design involves the variation of four factors (r , v , f , a) at three levels (3^4) and the factor (K_r) at two levels (2^1) conducted machining trials are completely based on design of experiments employing Taguchi's L_{18} orthogonal array associated with eighteen numbers of trial runs. The experimental design layout and results of machining trials are reported in Table 3.

3. Results and discussion

3.1 Development of predictive model using regression analysis

Based on the results of response characteristics obtained in accordance of Taguchi's L_{18} OA design of experiments were analysed in Minitab17 through multiple regression analysis and developed the best of empirical model to correlate between three machinability characteristics (surface finish of the machined component R_a , cutting force in FDHT process F_C , and flank wear of PVD-TiN coated Al_2O_3+TiCN mixed ceramic tool VB) with the given input machining parameters (K_r , V , f , a , r). Regression equations

for each response are presented by

$$F_c = -439.9 + 6.90K_r + 7.6r + 5.182V - 5672f + 447a - 0.192K_r*r - 0.06608K_r*V + 35.07K_r*f + 5.60 K_r*a - 0.247r*V + 2509r*f - 1047r*a + 3.865V*f + 3.525V*a - 2335f*a \quad (1)$$

$$R^2 = 99.9\%, R^2(\text{adj}) = 99.12\%$$

$$R_a = 2.665 - 0.0359K_r - 2.516r + 0.00438V + 9.45f - 5.83a + 0.03632K_r*r - 0.000032K_r*V + 0.0480K_r*f + 0.0199K_r*a - 0.00078r*V - 11.79r*f + 2.46r*a + 0.01145V*f - 0.00459V*a + 22.3f*a \quad (2)$$

$$R^2 = 99.93\%, R^2(\text{adj}) = 99.42\%$$

$$VB = -0.2707 + 0.004857K_r - 0.0456r + 0.000691V + 0.152f + 0.655a - 0.000505K_r*r - 0.000010K_r*V - 0.00579K_r*f - 0.002513K_r*a + 0.000608r*V + 0.773r*f - 0.2509r*a + 0.000647V*f + 0.000566V*a - 2.253f*a \quad (3)$$

$$R^2 = 99.98\%, R^2(\text{adj}) = 99.8\%$$

A comprehensive statistical analysis via analysis of variance (ANOVA) is performed depending upon results of cutting force, flank wear, and surface roughness obtained through machining experimentation, which represents a table containing degrees of freedom, sum as well as mean of squares (SS and MS), Fishers and probability values (F and P) and it is used to check as well as to determine a validity with significance of developed regression models for machinability parameters (F_C , R_a , and VB) and to evaluate the individual and interaction effects of different machining parameters on the corresponding response. Typically, the statistical significance is considered at 95% of confidence level, if the P-value is under 0.05 and the calculated F-value is above the standardized Fisher's value. From the Table 4a, it is observed that the developed models for cutting force (F_C) is significant along with the terms V , K_r*V , $r*f$, $r*a$, $V*f$, K_r are the influential parameters which has the pronounced nature on the response, F_C as their P-value and F-value justified the criterion of statistical significance. However, among all the considered machining variables, cutting speed presents the first position of influence (i.e., most significant) on cutting force. In the same context, the ANOVA result of surface roughness (R_a) model is presented in Table 4b, which shows the P-value is desirable (i.e., under 0.05), thereby resulting excellent significance of regression model. The factors, approach angle (K_r), nose radius (r), feed (f) along with two-way interaction terms (K_r*r , $r*f$) show the statistical significance to 5%. Besides, the interaction effect of nose radius-tool approach angle (K_r*r) along with individual effect of nose radius play the major roles associated with surface finish of the machined component. However, the factors such as cutting speed, depth of cut and interactions (K_r*V , K_r*f , K_r*a , $r*V$, $r*a$, $V*f$, $V*a$ and $f*a$) reflect insignificant impact on R_a , as their contributions are very inconsiderable. Similarly, the ANOVA result of tool's flank wear (VB) model is presented in Table 4c. Considering the criterion of significant level to 0.05, it is observed that the terms V , r , K_r , $r*V$, a , $r*f$, K_r*V , $f*a$ are the dominant contributors on flank wear evaluation of PVD-TiN coated Al_2O_3+TiCN

Table 4 ANOVA results for machinability parameters

(a) Cutting force (Fc) model						
Source	DF	Adj SS	Adj MS	F-Value	P-Value	Remarks
Model	15	36985.2	2465.68	127.96	0.008	Significant
Linear	5	12263.3	2452.67	127.96	0.008	Significant
Approach angle, Kr	1	6.8	6.82	0.35	0.612	
Nose radius, r	1	61.1	61.07	3.17	0.217	
Cutting speed, V	1	4464.4	4464.38	231.69	0.004	Significant
Feed, f	1	871.5	871.54	45.23	0.021	Significant
Depth of cut, a	1	4433.2	4433.20	230.07	0.004	Significant
2-way Interaction	10	8804.7	880.47	45.69	0.022	Significant
Kr*r	1	4.1	4.15	0.22	0.688	
Kr*V	1	3466.5	3466.55	179.91	0.006	Significant
Kr*f	1	900.2	900.20	46.72	0.021	Significant
Kr*a	1	140.5	140.51	7.29	0.114	
r*V	1	65.8	65.82	3.42	0.206	
r*f	1	1275.5	1275.49	66.20	0.015	Significant
r*a	1	678.8	678.80	35.23	0.027	Significant
V*f	1	363.5	363.48	18.86	0.049	Significant
V*a	1	495.8	495.83	25.73	0.037	Significant
f*a	1	74.2	74.22	3.85	0.189	
Error	2	38.5	19.27			
Total	17	37023.8				
(b) Surface roughness (Ra) model						
Model	15	4.27573	0.285049	196.06	0.005	Significant
Linear	5	1.26129	0.252258	137.51	0.006	Significant
Approach angle, Kr	1	0.00266	0.002656	1.83	0.309	
Nose radius, r	1	0.05751	0.057507	39.55	0.024	Significant
Cutting speed, V	1	0.02795	0.027951	19.23	0.048	Significant
Feed, f	1	0.40434	0.404339	278.11	0.004	Significant
Depth of cut, a	1	0.00671	0.006708	4.61	0.165	
2-way Interaction	10	0.39429	0.039429	27.12	0.036	Significant
Kr*r	1	0.14889	0.148886	102.41	0.010	Significant
Kr*V	1	0.00081	0.000810	0.56	0.533	
Kr*f	1	0.00168	0.001683	1.16	0.395	
Kr*a	1	0.00178	0.001785	1.23	0.383	
r*V	1	0.00066	0.000661	0.45	0.570	
r*f	1	0.02818	0.028177	19.38	0.048	Significant
r*a	1	0.00375	0.003747	2.58	0.250	
V*f	1	0.00319	0.003188	2.19	0.277	
V*a	1	0.00084	0.000842	0.58	0.526	
f*a	1	0.00679	0.006787	4.67	0.163	
Error	2	0.00291	0.001454			
Total	17	4.27864				
(c) Flank wear (VB) model						
Model	15	0.029694	0.001980	553.94	0.002	Significant
Linear	5	0.005023	0.001005	281.09	0.004	Significant
Approach angle, Kr	1	0.000517	0.000517	144.75	0.007	Significant
Nose radius, r	1	0.001074	0.001074	300.62	0.003	Significant
Cutting speed, V	1	0.003628	0.003628	1015.08	0.001	Significant
Feed, f	1	0.000009	0.000009	2.48	0.256	
Depth of cut, a	1	0.000203	0.000203	56.81	0.017	Significant
2-way Interaction	10	0.001657	0.000166	46.35	0.021	Significant
Kr*r	1	0.000029	0.000029	8.04	0.105	
Kr*V	1	0.000082	0.000082	22.96	0.041	Significant
Kr*f	1	0.000025	0.000025	6.87	0.120	
Kr*d	1	0.000028	0.000028	7.93	0.106	
r*V	1	0.000397	0.000397	111.10	0.009	Significant
r*f	1	0.000121	0.000121	33.92	0.028	Significant
r*a	1	0.000039	0.000039	10.89	0.081	
V*f	1	0.000010	0.000010	2.85	0.233	
V*a	1	0.000013	0.000013	3.57	0.199	
f*a	1	0.000069	0.000069	19.33	0.048	Significant
Error	2	0.000007	0.000004			
Total	17	0.029702				

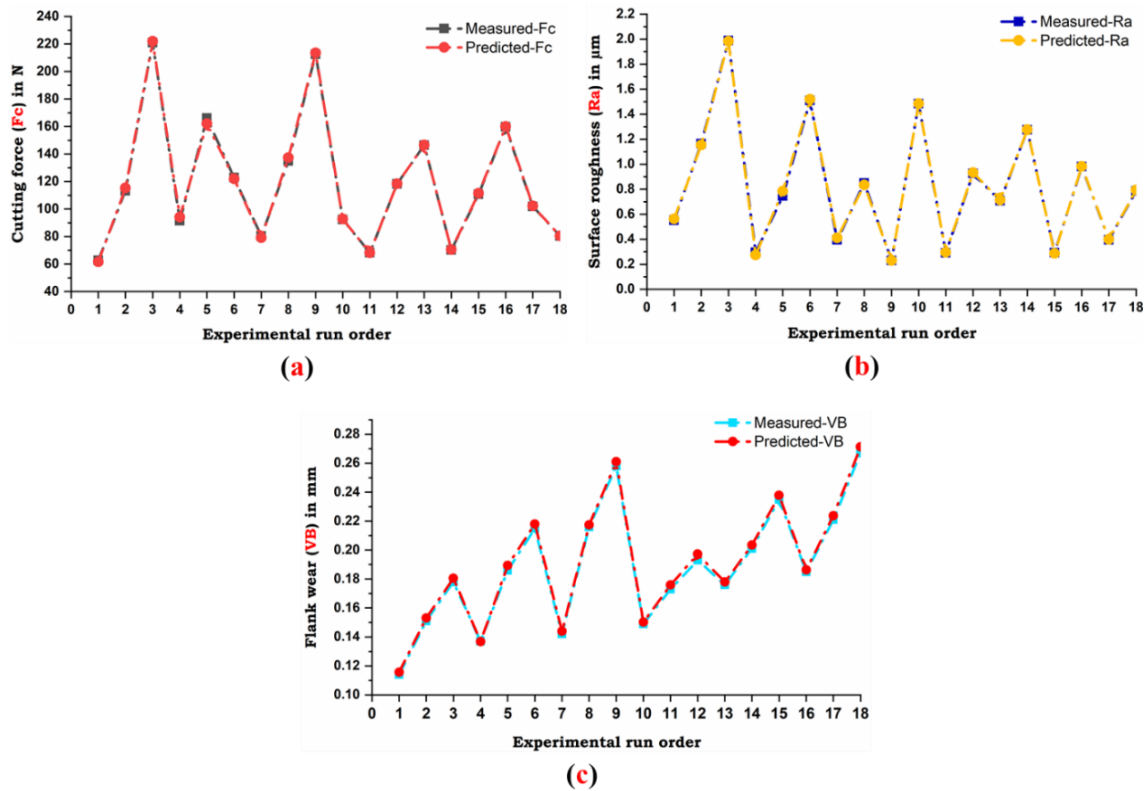


Fig. 4 Comparison between experimental and predicted values of machinability parameters: (a) cutting force, (b) surface roughness, and (c) flank wear

mixed ceramic tool which explain the larger calculated F-values (1015.08, 300.62, 144.75, 111.1, 56.81, 33.92, 22.96, 19.33, respectively) than standardized F-distribution value (18.51). It however affirms significance of the model and satisfies the significant interaction effect of nose radius and cutting speed on VB. However, the error percentage of contribution is very small (0.1% to Fc, 0.07% to Ra, and 0.02% in case of VB), means that no important factor has been missed or any large measurement error has been involved.

With the objective to avoid the misleading conclusion, several diagnostic tests such as adequacy, effectiveness and fit-of-data (i.e., goodness-of-fit) were performed for proposed regression models (Fc, Ra, VB). The calculated coefficient of determination, R² values (0.999, 0.9993, and 0.9998, respectively for Fc, Ra, VB) approaches to one better explained from the developed model using MRA for three machinability parameters (Fc, Ra, VB), which resembles goodness-of-fit for the model being statistically significant. Moreover, the predicted values are in good agreement with the experimental values which indicates the effectiveness of the model with greater predictability, as shown in Fig. 4. Finally, normal probability plot combined with Anderson-Darling test for Fc, Ra and VB confirm the acceptance of null-hypothesis criterion as shown in the Fig. 5. With lower AD-statistic (0.498 for Fc, 0.433 for Ra, and 0.158 in case of VB) as well as larger P-value (0.183 for Fc, 0.270 for Ra, and 0.941 in case of VB), concludes that the residuals are distributed falling on a straight line indicates

the normal distributed populations, justifies that the terms associated with the model are significant. In conclusion, the predictive models proposed for various technological performance characteristics using multiple regression analysis are effective in terms of adequate, statistically significant and probabilistically validate due to their higher R²-value, P-value less than 0.05 and larger AD-test P-value. Therefore, the proposed regression model can be effectively used for selection of objective function in multi-response optimization via. genetic algorithm followed by particle swarm optimization.

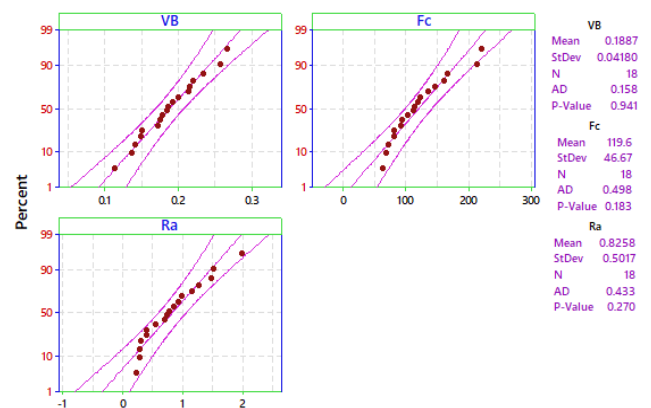


Fig. 5 Normal probability plot for machinability characteristics (VB, Fc, Ra)

3.2 Parametric influence on machinability characteristics

The effect of geometrical parameters (nose radius, approach angle) and cutting parameters (speed, feed, doc) on three major machinability parameters (F_c , R_a , VB) are graphically analyzed by three-dimensional (3D) surface plot. The typical 3D surface plot shown in Figure 6a illustrates the impact of two cutting variables (approach angle and nose radius) on principal cutting force (F_c). It is evident from Fig. 6(a) that cutting force (F_c) decreases with the increase in cutting tool approach angle. This possible outcome can be explained by the fact that, an approach angle of 90° or even higher, there is a tendency of higher shear angle and reduced chip thickness, leading to lower cutting force. Simultaneously, it conducts lower heat to the work and tool so that heat is concentrated at a reduced uncut chip width with a concentrated heat on smaller width of chip, and therefore a high temperature with low heat dissipation results thermal softening of workpiece material. Thus, cutting force (F_c) decreases. According to surface plot (Fig. 6(b)), as the insert's corner radius increases the cutting force increases. Zhao *et al.* (2017) reported the reason for this finding that increasing nose radius value reduces damping at elevated cutting speeds followed by the ploughing effect in the cutting zone that confirms the development of unreasonable cutting force. Fig. 6(c) predicts the increasing trend of cutting force value due to increase in feed and depth of cut. This effect is better explained due to the increase of tool-work contact area on the flank face and chip-tool contact area on the rake face of the cutting tool, which allows less contact time of machining for required material removal and for this reason, the amount of cutting force for chip deformation increases. This is in agreement with the findings of Gaitonde *et al.* (2009b).

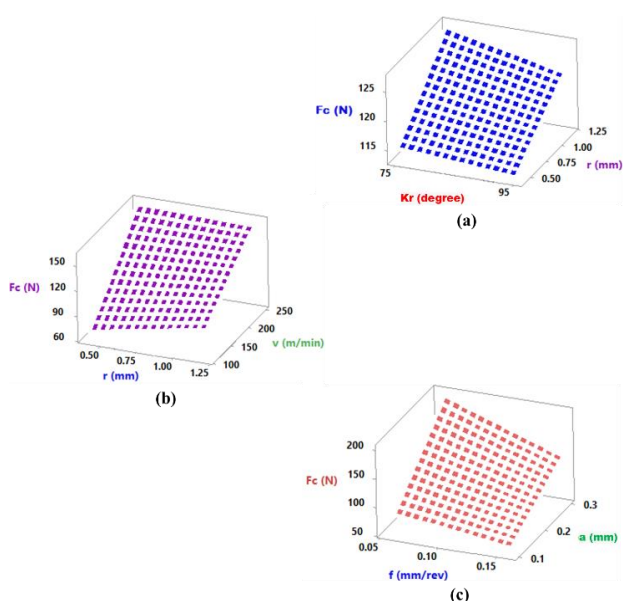


Fig. 6 Surface plots for illustration of machining parameters effect on cutting force

3D surface plot (Fig. 7(a)) shows the effect of approach angle and nose radius on surface roughness (R_a). Approach angle (K_r) exhibits a considerable effect on R_a . In fact, increasing the approach angle of work-tool combination, reduces cutting force due to controlled manner of plastic deformation followed by thermal softening and thus, contributes to improvement in surface finish. In addition, Fig. 7(a) shows the improvement in surface finish with the increase of edge corner radius of cutting tool. This is because of increasing the nose radius, the active cutting length of edge increases thus promoting better heat dissipation between tool and work, reducing heat concentration at the radius of the tool (Aouici *et al.* 2017). Fig. 7(b) shows magnificent variation on surface roughness with the rise in cutting speed possibly due to BUE formation (Khamel *et al.* 2012), material side flow (severe plastic deformation of machined surface) (Kishawy and Elbestawi 2001), and possibility of chatter (violent vibration of machine tool during cutting) (Sharma *et al.* 2008), leading to poor surface quality as the effect of tool wear is neglected. Also, the surface roughness increases with the increase in feed, as shown in Fig. 7(b). This phenomenon can be attributed to: (i) the formation of broader and deeper helicoid furrows on the machined surface (left by insert's nose-shape and the relative movement of workpiece-tool combination) by ploughing action (Kablouti *et al.* 2017), and (ii) well established relationship of geometrical arithmetic mean roughness with the cutting parameters, feed rate and corner radius of tool by the expression $R_a = 0.0321f^2/r$ (Shaw 2005, Davim and Figueira 2007, Das *et al.* 2015). Moreover, it is observed that, with increased feed rate under cutting condition ($K_r = 75^\circ$, $r = 1.2$ mm, $V = 110$ m/min, $a = 0.1$ mm) enhances vibration and heat generation with an evolution of undesirable thrust forces thereby resulting degraded surface finish, presented in Fig. 8. Apart, effect of doc seems to be insignificant on surface finish of machined part clearly shown in Fig. 7(c). Therefore, it is advisable to keep depth of cut in smaller value during hard turning to prevent chatter due to vibration, as reported by Suresh *et al.* (2012).

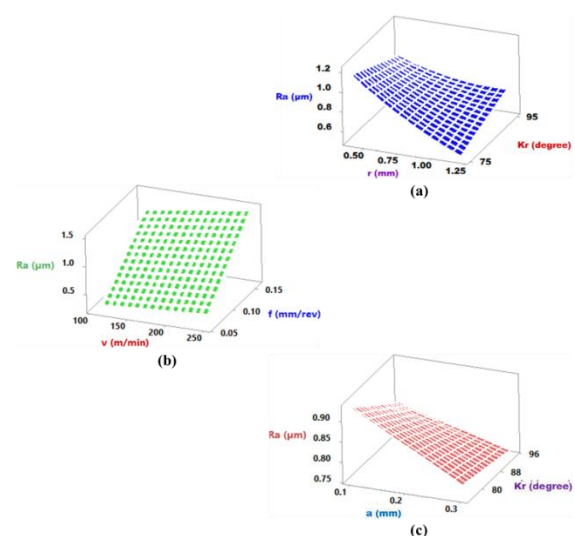


Fig. 7 Surface plots for illustration of machining parameters effect on surface roughness

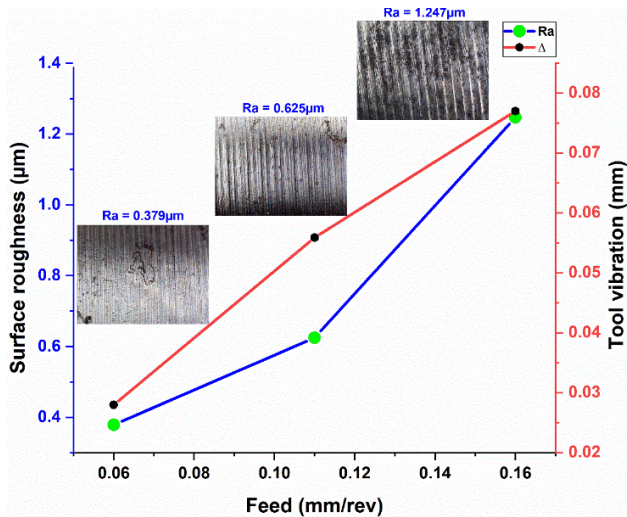


Fig. 8 Effect of feed on tool vibration and machined surface finish ($Kr = 75^\circ$, $r = 1.2$ mm, $V = 110$ m/min, $a = 0.1$ mm)

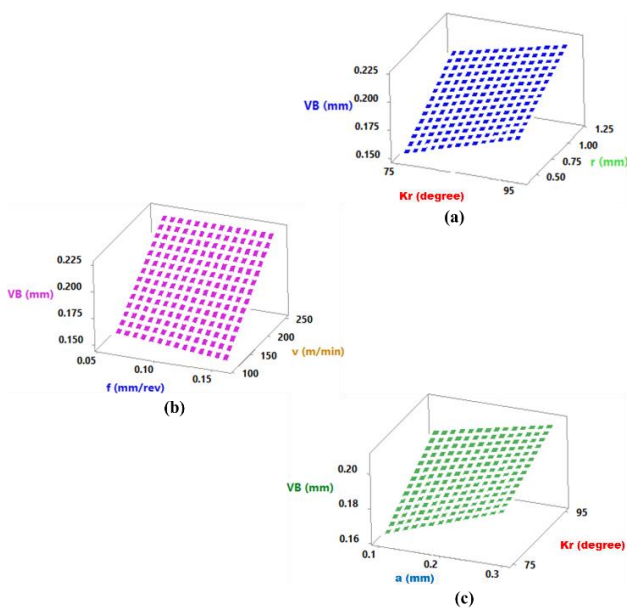


Fig. 9 Surface plots for illustration of machining parameters effect on tool's flank wear

For all turning tests, the measured Ra values were in the range of 0.23–1.998 μm , showing that coated ceramic tool is effective to produce components with surface corresponding to those obtaining from grinding and other finishing operations.

Tool wear variation with nose radius and approach angle is depicted in Figure 9. The response plot indicates that there is an increasing trend of flank wear (VB) with nose radius. It is obvious that larger nose radius is responsible for considerable deformation of the material under vicinity of the cutting edge, and provokes thermal as well as mechanical impacts due to friction and high interface temperature in the cutting zone thereby, increasing VB, as

earlier reported by Liu *et al.* (2004). From the diagram, it is also observed that extension in approach angle increases the cutting temperature, thereby leading to increased tool's flank wear, VB. According to surface plot (Fig. 9(b)), it has been found that increase in cutting speed tends to increase the flank wear nearly upto 0.3mm due to resulting higher cutting force, greater vibration, high temperature and heat generation at cutting zone, exceeds the thermal stability and yield strength of tool edge due to thermal softening of tool material along with severe rubbing effect between tool's flank side and machined surface contains hard constituents, and thus promote to intense tool wear (VB), as shown in Fig. 10. In the present study, the chips were generated in the region of tool nose (vicinity of cutting tool), as the range of cutting speed considered is less than nose radius of PVD-TiN coated $\text{Al}_2\text{O}_3+\text{TiCN}$ mixed ceramic tool. Increasing depth of cut extends the cutting edge angle, resulting increased arc length of machined region at work-tool interface. Under such condition, abrasion of ultra-hard carbide particles (Cr_7C_3 , VC, Mo_2C , Fe_3C) existing in the workpiece material accelerates the tool wear. Such variation of depth of cut on flank wear is clearly noticed Fig. 9(c).

Chips and its morphological aspects affect various machining attributes such as surface quality, tool life and machining temperature. Three types of chips are formed in hard machining; continuous type, segmented type and serrated type. In segmented type, prominent saw teeth are found without any shear band whereas in serrated chip, saw teeth with adiabatic shear band is observed. In the present experiment, both segmented chip and serrated chips were observed under dry cutting condition. Heat dissipation highly influenced the chip formation process in machining. Chips with better morphological characteristics formed with more heat dissipation. At higher cutting speeds temperature generation is more because of inadequate time for heat transfer. During FDHT, chips with prominent shear band (see, Fig. 11(a)), widely spaced saw tooth produced (refer, Fig. 11(b)) due to insufficient cooling.

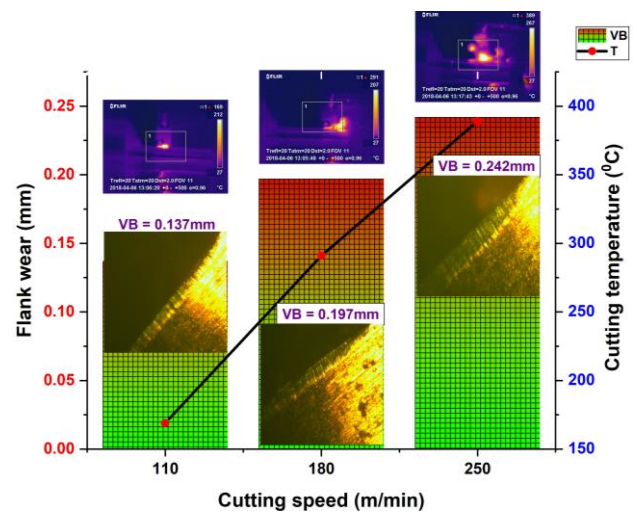


Fig. 10 Effect of cutting speed on cutting temperature and flank wear ($Kr = 75^\circ$, $r = 1.2$ mm, $f = 0.06$ mm/rev, $a = 0.1$ mm)

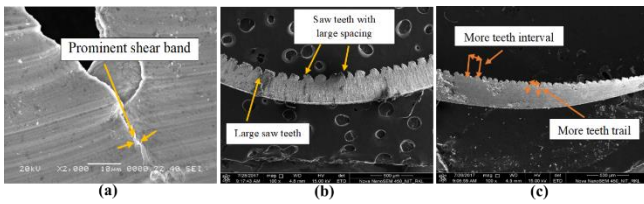


Fig. 11 Chip morphology (a) with shear band, widely spaced saw tooth (b), and saw teeth interval and trail (c)

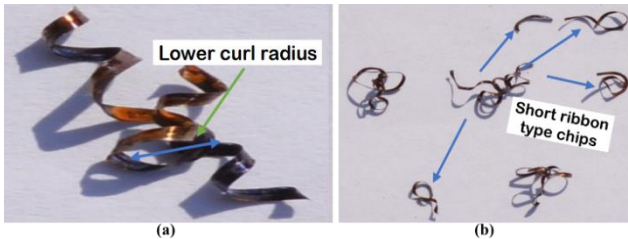


Fig. 12 Chips produced with short ribbon type with lower curl radius

And, chips with more teeth interval and trail is noticed, as shown in Fig. 11(c). Chip thickness, an important machining attribute, is highly influenced by tool life. More the tool wear, higher is chip thickness and less thickness are observed less tool wear. As reported by Das *et al.* (2019), with increase in feed the undeformed chip thickness increases. Consequently, tangential force increases as the shear plane area increases with increase in undeformed chip thickness. The formation of saw-tooth chip directly depends upon the thickness of undeformed chip i.e., increase in undeformed chip thickness leads to bigger saw-tooth. Chips with lower curl radius (see, Fig. 12) and short ribbon type chips are produced due to longer tool life which indicates chip breakability.

3.3 Optimization using response surface methodology

The present study includes multi-response optimization based on desirability function approach of RSM, to keep surface roughness of machined part, flank wear of cutting tool, and cutting force to minimum. Parameter design is an effective way to improve product quality as well as process efficiency. Desirability function approach is a statistical based multiple response robust parameter design methodology, employed for solving the multi-response optimization problems. The approach looks for correct combination of parameter levels that simultaneously takes the responsibility to fulfill the requirements placed on each response. The criterion for achievement of optimization result is evaluated based on overall desirability which is a weighted geometric mean of respective desirability for the different performance characteristics, expressed within the range of 0-1. Response will be completely unaccepted or undesirable if the desirability value approaches to 0. Response will be most desirable or accepted only if the

ideal desirability value is near or equal to 1.

For solving the parameter design problems by desirability function approach, the objective function, $F(x)$ is specified as (Costa *et al.* 2011);

$$F(x) = -DF$$

Overall (i.e., composite) desirability function can be stated as

$$DF = \left(\prod_{i=1}^n d_i^{w_i} \right)^{\frac{1}{\sum_{j=1}^n w_j}} \quad (4)$$

Here, DF is the composite desirability function which finds the optimal setting by minimizing the $F(x)$ (i.e., maximizes DF as it is highly desirable for optimization), d_i is the desirability designated for the i^{th} targeted output, and w_i is the weighting of d_i (considered equally important) in this study.

For a goal to minimization of output, individual desirability can be defined as

$$d_i = 1 \text{ if } Y_i \leq L_i$$

$$d_i = \left[\frac{H_i - Y_i}{H_i - L_i} \right] \text{ if } L_i \leq Y_i \leq H_i \quad (5)$$

$$d_i = 0 \text{ if } Y_i \geq H_i$$

where L_i and the H_i are respectively the lowest and largest acceptable value of Y for the i^{th} output response.

Fig. 13 shows optimization plot based on desirability function approach for machinability parameters showing the optimal manufacturing conditions for hard turning of AISI D3 steel with tool approach angle of 75° , nose radius of 1.2 mm, cutting speed of 110 m/min, feed rate of 0.06 mm/rev, doc of 0.1586 mm. The estimated optimum value of machinability characteristics are 62.665 N for F_c , 0.2557 μ m in case of R_a , and 0.1236 mm for VB .

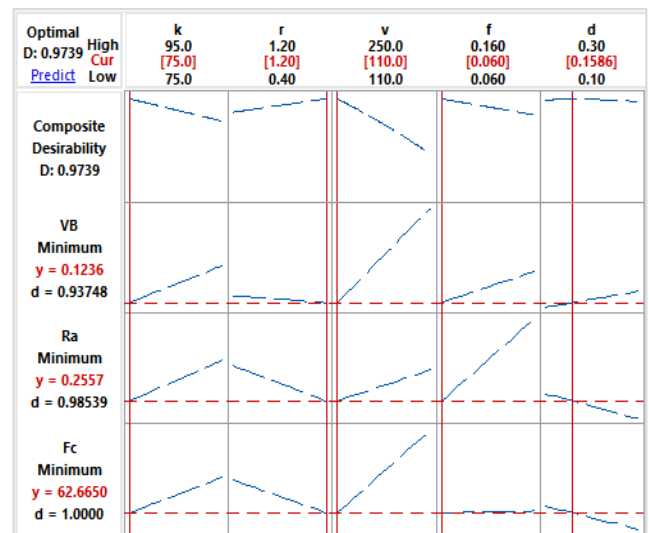


Fig. 13 Optimization plot for machinability parameters (F_c , R_a , VB) using desirability function approach

3.4 Optimization using genetic algorithm

In basic optimization procedure, the design space is actually so huge that it is not possible to work out a global optimum solution in a definite time period. Population based derivative free optimization like genetic algorithm (GA) is frequently employed to solve optimization problems stochastically that involve complexities like many conflicting aims, discrete, non-linear and non-convex domains. In GA, every possible solution is coded into genetic space wherein the search space is treated as a discrete function even though the same may be actually continuous. GA, a bio-inspired stochastic algorithm is effective in handling huge search area, evaluating the optimal solutions from a set of variables and constraints which might not have been negotiated in the entire lifetime otherwise. Concept wise, GA mimics the process of organic evolution and works on the 'survival of the fittest' logic. GA obtains the solutions by iteration, wherein the steps in the solutions are similar to chromosomes, a string of genes. Normally, GA is applied to problems where the fitness function can be well defined and the solutions can be degenerated into steps termed as chromosomes.

In GA, a set of genetic operators bring about diversity required for evolution process. The algorithm progresses through three genetic operators such as selection, crossover (mating) and mutation. The selection operator involves survival of the fittest and struggle for the existence, by choosing the chromosomes as parents for mating (crossover) and produce offspring. Selection implies creating a subset of genes from an existing population set. Every gene has a quality measure and fitness function attached to it. Fitness function is an indicator of an optimization solution and illustrates the proximity of a given solution to the intended outcome. Crossover operator is the principal factor that involves mating of two chromosomes to yield a new offspring. It is likely that the new chromosome can be better than both its parents if it inherits the best attributes from each of the parents. Mutation is a biological random process followed after crossover operation where forcefully some chromosomes are modified to get a better solution. Mutation operator gives mobility to the population and is an important part of the generic search. The abovementioned process operators continue in a repetitive way while waiting for the chromosomes have the optimum or the best fitness solution for a certain optimization problem is attained. Once the new generation is completed, it is evaluated again and checked experimentally by confirmation test for approval and agreement. Fig. 14 shows the flow chart of GA technique that works to address the optimization problem.

The present study includes multi-response optimization based on computational approach by genetic algorithm, to keep surface roughness of machined part, flank wear of cutting tool, and cutting force in hard turning to minimum. In finish dry hard turning, multi-response optimization problem of GA is defined as follows

Find: input parameters (Kr, r, V, f, a) (6)

Minimize: Y(Fc, Ra, and VB) (7)

Allowable range of process parameters are: $75^\circ \leq$ approach angle (Kr) $\leq 95^\circ$, $0.4 \text{ mm} \leq$ nose radius (r) $\leq 1.2 \text{ mm}$, $110 \text{ m/min} \leq$ cutting speed (V) $\leq 250 \text{ m/min}$, $0.06 \text{ mm/rev} \leq$ feed rate (f) $\leq 0.16 \text{ mm/rev}$, and $0.1 \text{ mm} \leq$ depth of cut (d) $\leq 0.3 \text{ mm}$ (8)

Earlier in this study, the models Eqs. (1)-(3) developed by multiple regression analysis respectively for cutting force, surface roughness, and flank wear are considered as objective functions Y(Fc), Y(Ra), and Y(VB) for mathematical description in GA optimization. Fig. 15 represents the optimization history via Pareto plot, which proposes to minimize the three machinability parameters (Fc, Ra, VB) of hard turning with reference to algorithm-critical parameters of GA.

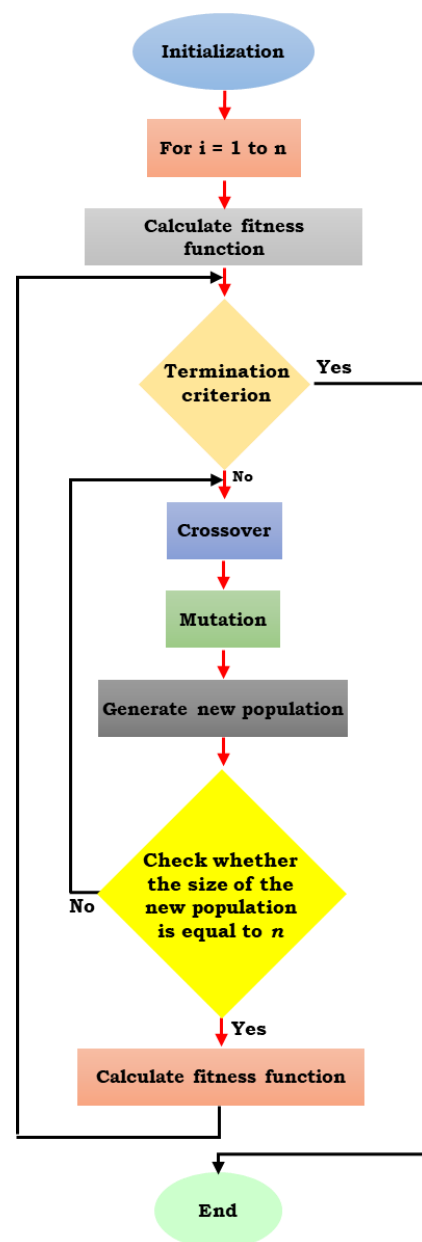


Fig. 14 Flow chart of GA-based algorithm

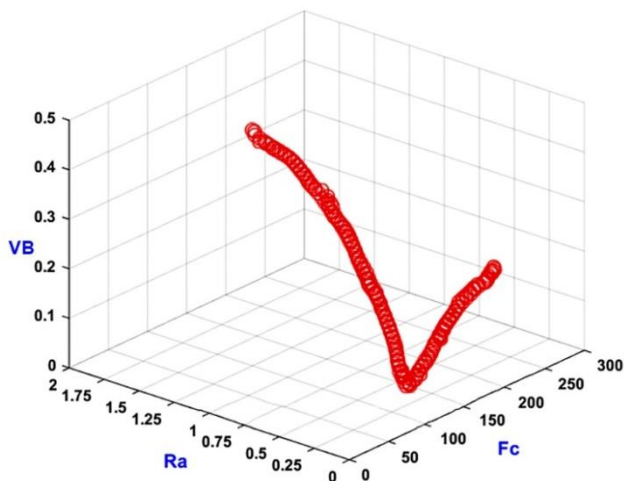


Fig. 15 GA based Pareto plot during optimization

By solving the multi-response optimization problem with GA technique, the optimized manufacturing conditions for hard turning of AISI D₃ steel are obtained with tool approach angle of 75°, nose radius of 1.2 mm, cutting speed of 117 m/min, feed rate of 0.06 mm/rev, doc of 0.3 mm. Finally, the estimated optimal values of pre-cited three machinability parameters are 51.356 N for Fc, 0.1833 μm in case of Ra, and 0.144 mm for VB.

3.5 Optimization using PSO

Particle swarm optimization (PSO) is a stochastic based computational method inspired by socio-biological behaviour of fish schooling and bird flocking, which considers intelligent search strategy in population to achieve the new global best solution. In PSO technique, the population called as swarm moves around the search space to find a possible solution with less computational effort. Iterations in PSO enable each particle to have personal best solution followed by global best position of any particle in the swarm. When such promising solution is unearthed by a particle, other particles in the search region are in close proximity to it. Therefore, such a method ensures a potential solution for each particle termed as 'bird'. In order to measure the goodness of fitness value of all the particles in the swarm mainly depends on simple mathematical formulae over particle's position and velocities, that quantifies the quality of a potential solution. The ability of birds to fly collectively within search space are therefore influenced by neighboring particles discovering optimal regions. After initializing a group of random particles, search for optima is calculated by updating generations by two best values such as personal best (p_{best}) and global best (g_{best}). Each particle consists of data representing a possible solution. The p_{best} value indicates the closeness of particle's data towards the target. It is common to see PSO algorithms use neighborhoods that helps the algorithm to avoid getting stuck in local minima. For PSO calculations, two major parameters are considered like particle velocity and position, which are updated after each iteration and solution

moves ahead towards best possible results. The PSO algorithm comprises of following steps: (i) initiate invariable distribution of particles, (ii) every particles position is assessed by a objective function, (iii) particle's position is updated with better solution, (iv) previous best positions finalizes the best particle, (v) particle's velocity is updated, (vi) new positions of the particle are encountered after updating, and (vii) move to step 2 until stopping criteria is satisfied (i.e., until the optimum solution is obtained).

During each iteration, present particle position and velocity are updated using the following two equations

$$v_i^{k+1} = wv_i^k + C_1R_1(p_{best_i} - x_i^k) + C_2R_2(g_{best} - x_i^k) \quad (9)$$

$$x_i^{k+1} = x_i^k + v_i^{k+1} \quad (10)$$

where, v_i^k and x_i^k respectively represents the velocity and location of i^{th} particle at iteration k^{th} in reference to search space of N-dimension; C_1 & C_2 respectively are the cognitive and social learning factors; R_1 and R_2 are random coefficients usually between 0 and 1; p_{best_i} & g_{best} represents the best position of i^{th} particle and swarm, respectively; w is the inertia weight coefficient can be defined as follows

$$w = w_{max} - \left[\frac{w_{max} - w_{min}}{iter_{total}} \times iter_{current} \right] \quad (11)$$

where, w_{min} & w_{max} are the minimum and maximum inertia weights; and $iter_{current}$ & $iter_{total}$ are the current iteration and total number of iterations used in PSO to assign an optimal solution.

In this study, PSO technique is best suited for multi-response optimization with the purpose to minimize the surface roughness of hard turned component, flank wear of cutting tool, and cutting force in hard turning. For this reason, the models Eqs. (1)-(3) developed by multiple regression analysis, respectively for Fc, Ra, and VB are employed for mathematical description of combined objective function called global minimum ($Z_{GLOBALMIN}$) as given by Eq. (12).

$$Z_{GLOBALMIN} = W_1 * \frac{F_c}{F_{c_{min}}} + W_2 * \frac{R_a}{R_{a_{min}}} + W_3 * \frac{VB}{VB_{min}} \quad (12)$$

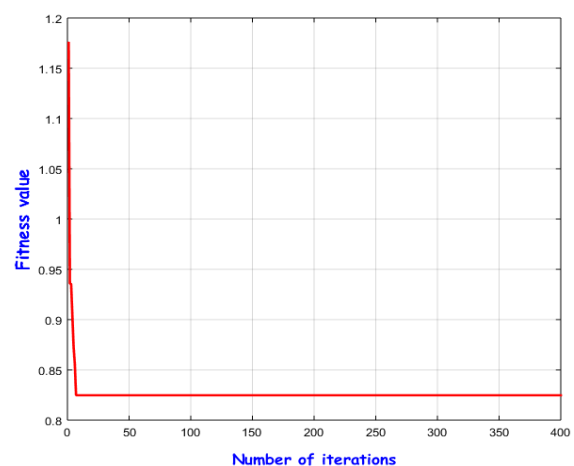


Fig. 16 Convergence plot during optimization via. PSO

Table 5 Overview of confirmatory experiments and comparison of results

Methods	Optimum machining parameters					Cutting force, Fc (N)		Surface roughness, Ra Flank wear, VB (mm)		Average error (%)		
	Kr	r	V	f	a	Pred.	Expt.	Pred.	Expt.	Pred.	Expt.	
RSM	75	1.2	110	0.06	0.1586	62.665	52.37	0.2557	0.225	0.1236	0.143	15.62%
GA	75	1.2	117	0.06	0.3	51.356	58.55	0.1833	0.21	0.144	0.156	10.89%
PSO	75	1.2	110	0.06	0.3	42.823	47.68	0.181	0.207	0.138	0.141	8.29%

Here, W_1 (0.33), W_2 (0.34), and W_3 (0.33) are the individual weight assigned corresponding to the responses Fc, Ra, VB, respectively, whose sum of their weights is 1. Figure 16 represents the optimization history via convergence plot, which proposes to minimize the three machinability parameters (Fc, Ra, VB) of hard turning with PSO-specific parameters. By solving the multi-response optimization problem with PSO technique, the optimal manufacturing conditions for hard turning of AISI D3 steel are obtained with tool approach angle of 75° , nose radius of 1.2 mm, cutting speed of 110 m/min, feed rate of 0.06 mm/rev, doc of 0.3 mm. Finally, the estimated optimal values of pre-cited three machinability characteristics are 51.356 N for Fc, 0.1833 μm in case of Ra, and 0.144 mm for VB.

3.6 Confirmation test

With a view to avoid misleading conclusion, the optimum machining conditions suggested by RSM, GA and PSO techniques are validated with the results of confirmation test, which could be possible by conducting three additional experiments using the same experimental setup. Further, the results obtained from above mentioned three optimization techniques are compared against each other to check, illustrate and verify the effectiveness as well as improvement in predicting the machinability characteristics (Fc, Ra, VB) in during FDHT process. A comparison between the optimal and experimental values of responses (Fc, Ra, VB) under the cutting conditions proposed by RSM, GA and PSO is presented in Table 5. The results of PSO approach present the best combination of process parameters for optimization of cutting force, surface roughness and tool wear because, the error percentage in the case of PSO (8.29%) is lower than that obtained via GA (10.89%) and RSM (15.62%). Hence, PSO method is chosen for economic analysis.

3.7 Estimation of energy and carbon footprint savings

In response to cost consciousness for economical hard turning, reduction in energy consumption is of great importance as it leads to paradoxical improvement of savings in production cost. Energy crisis and environmental issue have become increasingly popular concerns for every industry in the world in terms of sustainable development. Yet, the customers increasing pressure for desired product quality has led to improved surface finish and hence the

energy consumption has also increased. The higher use of energy has thereby led to higher emission of CO_2 . It is a strong concern, especially in emerging as well as developing economies to improve manufacturing efficiency so as to reduce material & energy consumption, and industrial pollution for sustainable performance of machining processes. At the same time, proper selection of process parameters in machining is of prime importance with a view to achieve better product quality, high productivity and low cost.

For the determination of energy consumption during hard turning, the cutting power (P) is calculated with measured results of cutting force from the confirmation test by using the formula; $P = Fc \times V$. Thereafter, the reduction in energy consumption followed by the estimation of carbon foot print saved are calculated by determining the difference under optimized and non-optimized cutting conditions. The result presented in Table 6 expresses the amount of energy as well as carbon footprints saved in kWh and kg, respectively.

According to the Ministry of Energy in India, one unit (i.e., 1 kWh) of electricity = 0.523 kg of CO_2 emission. It is observed that, hard turning with appropriate machining conditions undertake the considerable reduction in the energy consumption and enhancement in savings of carbon footprints, which finds the benefits from ecological as well as economical point of views

3.8 Economical analysis

Cost consciousness with respect to machining process is fundamental venture of efficient manufacturing system. In order to determine manufacturing costs for a machining operation, important criteria are selected based on convolution of shape, product accuracy and tooling process. Nowadays, profitability and cost management emphasized manufacturers to control the entire expenditure for machining operation in order to establish consistency and confirm recommended cost benchmarks for the future. Due to the large expenditures involved, it is necessary to analyze machining operations in order to operate with optimum economic conditions. For components produced by machining, cost estimation is kept minimum by considering optimum tool life and total machining cost per part. Longer tool life results in high cost of labor, the cost of machining operation, the overhead costs and makes the operation costly because the time of completion of the operation increases. On the other hand, shorter tool life instigates high tool cost, the tool resetting cost, and machine downtime

Table 6 Estimation of energy and carbon footprints saved

Total amount of operational time for the lathe machine per annum	Energy consumption during each similar operation with standard inputs	Total energy consumed per annum	Energy consumption during machining operation with optimized parameters	Total energy consumed per annum at optimized condition	Amount of energy saved per annum	Carbon footprints saved (kg of CO ₂)
655hrs.	115 Watts	$115 \times 3,600 \times 655 = 271170000$ Joule	$42.823 \times 110 = 78.51$ Watts	$78.51 \times 3,600 \times 655 = 185126580$ Joule	86043420 Joule or 86043.42 kWh \approx 31.73%	45000.71

because of frequent change of cutting tools caused by the rapid wear of cutting tool. Thus, a trade-off standard for selection of suitable combination of machining parameters must be determined based on the cost and quality considerations. At the same time, machining parameters will definitely affect the production rate as well as production cost. Again, tool life becomes significant in this context since the cost of the tools influences the machining cost considerably. All these things make the costing process more complicated to arrive at an optimum process. In machining process, this can only be possible by estimating tool life at optimized cutting conditions.

For this reason, an additional experiment is performed with same setup at best optimal cutting conditions as suggested by PSO technique for assessing the tool life of the PVD-TiN coated Al₂O₃+TiCN mixed ceramic cutting insert by considering the control limit criterion of flank wear (VB) upto 0.3 mm. Figure 17 shows a typical graph of progress of flank wear, VB with cutting time upto tool life of 41 min for PVD-TiN coated Al₂O₃+TiCN mixed ceramic tool. Considering estimated tool life, Gilbert's approach [45] is used to perform detailed direct and indirect cost estimation in terms of total machining cost per part, shown in Table 7.

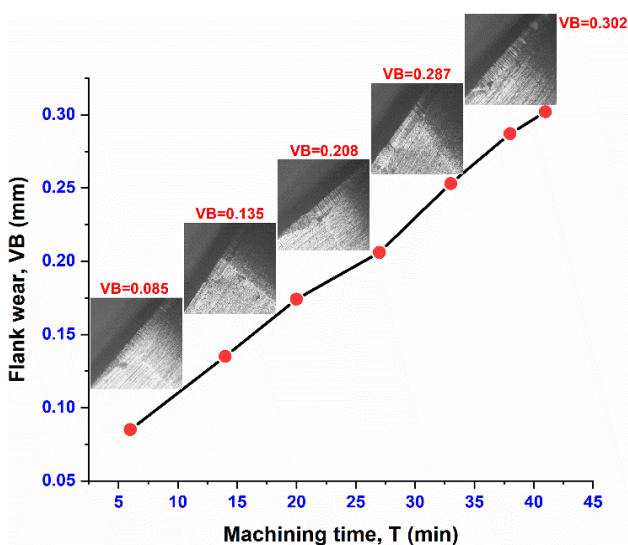


Fig. 17 Growth of flank wear with machining time under the best optimum cutting condition obtained by PSO

Table 7 Cost estimation in FDHT of AISI D3 steel with PVD-TiN coated Al₂O₃+TiCN mixed ceramic tool

Sl. no.	Costs	In Indian rupees (Rs.)
1	Machine and labour cost (x), Rs.600/h	Rs.10/min
2	Cutting cost per component (xT_m)	Rs.25
3	Tool changing cost per component [$xT_d(T_m/T)$]	Rs.3.05
4	Cost of each tool	Rs.1100
5	Mean cost of the cutting tool edge (y)	Rs.275
6	Tooling cost per component [$y(T_m/T)$]	Rs.16.77
7	Total cutting cost per component, (2+3+6)	Rs.44.82

Axial length of workpiece to be cut (L)= 150 mm, finish diameter of workpiece (D)= 35 mm, time for machining the part (T_m)= $(\pi DL/1000Vf) = 2.5$ min, measured tool life (T) for single cutting edge at optimum machining condition ($K_r = 75^0$, $r = 1.2$ mm, $a = 0.3$ mm, $f = 0.06$ mm/rev, and $V = 110$ m/min) = 41 min, machine downtime (T_d)= 5 min

It is noticed that the total machining cost per part using coated PVD-TiN coated Al₂O₃+TiCN mixed ceramic inserts is considerably lower around Rs.44.82. It is interesting to note that the cost estimation of operational activities in FDHT process ensures a dramatic gain in productivity and efficiency in finish hard turning. The cheapest solution to have lower tool cost and total cost of the part as longer tool life with minimized downtime calculations is obtained using PVD-TiN coated Al₂O₃+TiCN mixed ceramic inserts that justifies an economic solution to finish machining of hardened parts.

3.9 Sustainability assessment

Sustainable assessment of every production technology is very prominent perspective, prior to its adoption in industry for safer and cleaner manufacturing. The term "sustainable manufacturing" encourages adopting new environmental-friendly technologies as well as economically-sound processes with a broader social implication which promotes eliminating production and processing wastes, minimizes negative environmental impacts while conserving energy, and enhances employee health and safety through eco-efficient practices. Sustainable manufacturing is effective to justify the existence of production methodology by various parameters such as production cost and rate, cutting quality, process management, water and energy intensity, material waste

management, environmental regulation, worker health and safety, labour relations, training and education. In the present work, sustainability assessment of hard turning process under dry environment condition is performed concerning technological, economical, and ecological aspects. For this, a decision-making effective technique called Pugh matrix is employed for sustainability assessment by assigning specific weight in terms of mathematical number for the abovementioned sustainable manufacturing parameters. The weight criteria are allocated to each quality parameter in the range from -2 to 2 based on its importance (i.e., superior or inferior results).

In the present study sustainability of finish dry hard turning process is assessed by considering environmental effect, operator health, coolant cost, waste management, surface roughness, actual machining cost, energy consumption related to CO₂ emission. In this context, environmental effect and coolant cost is given weightage “2” whereas others are assigned with an equal weightage “1”. During dry hard turning, cutting without coolant provides obvious cost benefits. Therefore, the score of “2” is provided to the coolant cost. Without using the cutting fluid, the operator health and environment is free from any harmful effects eligible to obtain score of “2” as well. Apart, hazards faced by the operator in the machine area involves carrying away of chips and parts fly off during production, makes the score “-1”. As there is no pollution, no disposal cost and no danger of health due to absence of cutting fluid, minimization of waste and spill over during production obtains a score “1”. Such machining process utilizes less coolant thereby causing no wetting of the workpiece. A little amount of labour is sufficient for machine cleaning. Dry cutting implies smoother finish as well as less production cost which adds a score “1” towards machining cost, and surface roughness. Moreover, at appropriate settings of cutting parameters dry hard turning is economically viable to justify the savings of energy via. less greenhouse gas (i.e., carbon footprint) emission. After calculation, a total score of “5” is obtained which is reflected in Kiviati diagram, as shown in Fig. 18. In brief, dry hard turning is practically viable in terms of sustainability providing better surface roughness, improved economic and socio-technological benefits. However, to make such a decision, further investigation is required.

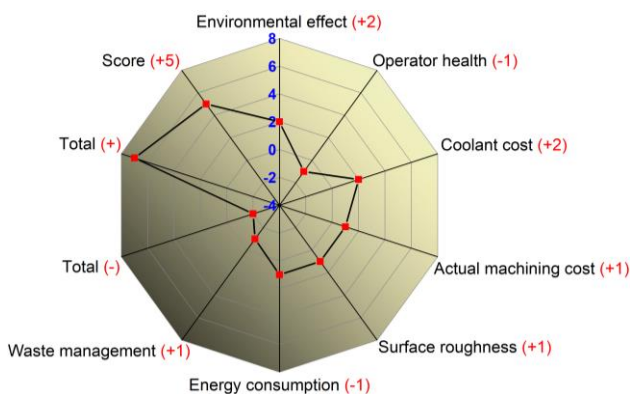


Fig. 18 Pugh matrix associated with Kiviati diagram for sustainability assessment

5. Conclusions

On the basis of experimental results obtained during FDHT of AIS D3 steel with PVD-TiN coated Al₂O₃+TiCN mixed ceramic tool, various conclusions are drawn as follows:

- The contribution of nose radius followed by the interaction effects of approach angle-nose radius, and last by cutting speed-nose radius found to be the most significant for the improvement of surface finish, and achieved the roughness (R_a) in the range of 0.23–1.988 μ m.
- Contrary to presumed knowledge the cutting speed, not depth of cut, principally as well as significantly affected the cutting force (F_c), followed by the interaction effect of parameters approach angle-cutting speed, and feed.
- The statistical analysis based on the technique of ANOVA followed by the surface effect plot reported that, the cutting speed is the most influential parameter for control on tool wear (VB). Although, the influence of depth of cut has not been observed statistically significant, but the flank wear is an increasing function of depth of cut.
- In serrated type chips, a widely spaced saw tooth with adiabatic shear band due to insufficient cooling are observed at high cutting speed.
- The predictive models proposed for various machinability parameters using multiple regression analysis are effective in terms of adequate, statistically significant and probabilistically validate due to their higher R²-value (0.999 for F_c , 0.9993 for R_a , 0.9998 in case of VB), P-value less than 0.05 (0.008 for F_c , 0.005 for R_a , 0.002 in case of VB) and larger AD-test P-value (0.183, 0.27, 0.941, respectively for F_c , R_a , VB).
- By solving the multi-response optimization problem with RSM's desirability function analysis, the optimal manufacturing conditions for hard turning are obtained at tool approach angle (K_r) of 75°, nose radius (r) of 1.2 mm, cutting speed (V) of 110 m/min, feed rate (f) of 0.06 mm/rev, doc (a) of 0.1586 mm. The estimated optimum value of machinability parameters are 62.665 N for F_c , 0.2557 μ m in case of R_a , and 0.1236 mm for VB.
- The application of genetic algorithm (GA) for multi-response optimization presented the optimal manufacturing conditions of the input variables were $K_r= 75^\circ$, $r= 1.2$ mm, $V= 117$ m/min, $f= 0.06$ mm/rev, and $a= 0.3$ mm. The optimum response values are 51.336 kN, 0.1833 μ m, and 0.144 mm for F_c , R_a , and VB, respectively.
- The results derived from the multi-response optimization technique via. PSO show the best optimal manufacturing conditions for hard turning of AISI D₃ steel at $K_r= 75^\circ$, $r= 1.2$ mm, $V= 110$ m/min, $f= 0.06$ mm/rev, and $a= 0.3$ mm. The optimum response values are 42.82 kN, 0.181 μ m, and 0.138 mm for F_c , R_a , and VB, respectively.
- At best optimal conditions (suggested by PSO technique), the tool life of PVD-TiN coated mixed (Al₂O₃ + TiCN) ceramic insert is found to be 41 min under the consideration of flank wear (VB) criterion

limit upto 0.3mm and estimated the total machining cost per component of only Rs.44.82 in Indian rupees, which ensures benefit from economical point of view because of longer tool life and reduced machine downtime.

- Under optimized machining conditions, the consumption of energy is reduced by 31.73% which lowers the cost of machining by improving the energy savings and reduced the CO₂ gas emission, promising towards green manufacturing and clean production for the manufacturing industry.
- During FDHT of hardened AISI D3 steel by coated PVD-TiN coated Al₂O₃+TiCN mixed ceramic tool, use of cutting fluid becomes optional when strict environmental laws are imposed and provides techno-economical, and ecological advantages.
- Machining with dry environment condition, sustainability assessment results in overall improvement in turn reduces the ecology and health related problems, the cost of machining by eliminating the cutting fluid consumption and cost related to the carrying and disposal of cutting fluid, increase the production rate by reducing the time taken for in house-keeping of the machine, shop floor and handling of wet chips.
- To substitute of costlier CBN and PCBN tools, PVD-TiN coated Al₂O₃+TiCN mixed ceramic tools can be preferred to bring high levels of productivity for the shaft and die making industry in finish hard turning operations hardness ranging from 45-65HRC, especially, PVD-TiN coating with excellent wear resistance.
- Optimized cutting parameters are evaluated that contributes to machining-end outcomes in terms of surface finish improvement close to that obtained in grinding, tool wear reduction along with cutting force minimization.
- The proposed multiple techniques (Taguchi's OA-MRA-RSM-GA-PSO) demonstrate an effective approach towards improvement in hard turning operation and it can be implemented in real-time process monitoring, predictive model control and optimization during machining of different workpiece materials as well as in other machining processes via. advances in computer technology.

The research findings from the machinability investigation and sustainability assessment would be a good technical database for the aerospace, automobile and military applications in machining aspects applicable to hard-to-cut materials.

References

Anand, A., Behera, A.K. and Das, S.R. (2019), "An overview on economic machining of hardened steels by hard turning and its process variables", *Manufact. Rev.*, **6**, 4. <https://doi.org/10.1051/mfreview/2019002>.

Aouici, H., Bouchelaghem, H., Yallese, M.A., Elbah, M. and Fnides, B. (2014), "Machinability investigation in hard turning of AISI D3 cold work steel with ceramic tool using response surface methodology", *Int. J. Adv. Manufact. Technol.*, **73**(9-12), 1775-1788. <https://doi.org/10.1007/s00170-014-5950-0>.

Aouici, H., Khellaf, A., Smaiah, S., Elbah, M., Fnides, B. and

Yallese, M.A. (2017), "Comparative assessment of coated and uncoated ceramic tools on cutting force components and tool wear in hard turning of AISI H11 steel using Taguchi plan and RMS", *Sādhanā*, **42**(12), 2157-2170. <https://doi.org/10.1007/s12046-017-0746-1>.

Asiltürk, İ. (2012), "Predicting surface roughness of hardened AISI 1040 based on cutting parameters using neural networks and multiple regression", *Int. J. Adv. Manufact. Technol.*, **63**(1-4), 249-257. <https://doi.org/10.1007/s00170-012-3903-z>.

Astakhov, V.P. (2011), *Machining of Hard Materials – Definitions and Industrial Applications*, In: J. Paulo Davim (ed.), *Machining of Hard Materials*. Springer-Verlag, London, 1-32.

Bartarya, G. and Choudhury, S.K. (2013), "Influence of machining parameters on forces and surface roughness during finish hard turning of EN 31 steel", *Proceedings of the Institution of Mechanical Engineers, Part B: J. Eng. Manufact.*, **228**(9), 1068-1080.

Benlahmidi, S., Aouici, H., Boutaghane, F., Khellaf, A., Fnides, B., and Yallese, M. (2016), "Design optimization of cutting parameters when turning hardened AISI H11 steel (50 HRC) with CBN7020 tools", *Int. J. Adv. Manufact. Technol.*, **89**(1-4), 803-820. <https://doi.org/10.1007/s00170-016-9121-3>.

Bensouilah, H., Aouici, H., Meddour, I., Yallese, M.A., Mabrouki, T. and Girardin, F. (2016), "Performance of coated and uncoated mixed ceramic tools in hard turning process", *Measurement*, **82**, 1-18. <https://doi.org/10.1016/j.measurement.2015.11.042>.

Bouacha, K., Yallese, M.A., Khamel, S. and Belhadi, S. (2014), "Analysis and optimization of hard turning operation using cubic boron nitride tool", *Int. J. Refractory Metals Hard Mater.*, **45**, 160-178. <https://doi.org/10.1016/j.ijrmhm.2014.04.014>.

Bouacha, K. and Terrab, A. (2016), "Hard turning behavior improvement using NSGA-II and PSO-NN hybrid model", *Int. J. Adv. Manufact. Technol.*, **86**(9-12), 3527-3546. <https://doi.org/10.1007/s00170-016-8479-6>.

Bouaid, L., Yallese, M.A., Chaoui, K., Mabrouki, T. and Boulouar, L. (2014), "Mathematical modeling for turning on AISI 420 stainless steel using surface response methodology", *Proceedings of the Institution of Mechanical Engineers, Part B: J. Eng. Manufact.*, **229**(1), 45-61. <https://doi.org/10.1177/0954405414526385>.

Chinchankar, S. and Choudhury, S.K. (2013), "Investigations on machinability aspects of hardened AISI 4340 steel at different levels of hardness using coated carbide tools", *Int. J. Refractory Metals Hard Mater.*, **38**, 124-133. <https://doi.org/10.1016/j.ijrmhm.2013.01.013>.

Costa, N.R., Lourenço, J. and Pereira, Z.L. (2011), "Desirability function approach: A review and performance evaluation in adverse conditions", *Chemometrics Intel.Laboratory Syst.*, **107**(2), 234-244. <https://doi.org/10.1016/j.chemolab.2011.04.004>.

Das, A., Mukhopadhyay, A., Patel, S.K. and Biswal, B.B. (2016), "Comparative assessment on machinability aspects of AISI 4340 alloy steel using uncoated carbide and coated cermet inserts during hard turning", *Arabian J. Sci. Eng.*, **41**(11), 4531-4552. <https://doi.org/10.1007/s13369-016-2160-0>.

Das, A., Patel, S.K., Hotta, T.K. and Biswal, B.B. (2018), "Statistical analysis of different machining characteristics of EN-24 alloy steel during dry hard turning with multilayer coated cermet inserts", *Measurement*, **134**, 123-141. <https://doi.org/10.1016/j.measurement.2018.10.065>.

Das, A., Tirkey, N., Patel, S.K., Das, S.R. and Biswal, B.B. (2019), "A comparison of machinability in hard turning of EN-24 alloy steel under mist cooled and dry cutting environments with a coated cermet tool", *J. Fail. Anal. Prevention*, **19**, 115-130. <https://doi.org/10.1007/s11668-018-0574-6>.

Das, S.R., Dhupal, D. and Kumar, A. (2015), "Experimental investigation into machinability of hardened AISI 4140 steel

- using TiN coated ceramic tool”, *Measurement*, **62**, 108-126. <https://doi.org/10.1016/j.measurement.2014.11.008>.
- Davim, J.P. and Figueira, L. (2007), “Comparative evaluation of conventional and wiper ceramic tools on cutting forces, surface roughness, and tool wear in hard turning AISI D2 steel”, *Proceedings of the Institution of Mechanical Engineers, Part B: J. Eng. Manufact.*, **221**(4), 625-633. <https://doi.org/10.1243/09544054JEM762>.
- Davim, J.P. and Figueira, L. (2007), “Machinability evaluation in hard turning of cold work tool steel (D2) with ceramic tools using statistical techniques”, *Mater. Design*, **28**(4), 1186-1191. <https://doi.org/10.1016/j.matdes.2006.01.011>.
- Fnides, B., Aouici, H., Elbah, M., Boutabba, S. and Boulanouar, L. (2015), “Comparison between mixed ceramic and reinforced ceramic tools in terms of cutting force components modelling and optimization when machining hardened steel AISI 4140 (60 HRC)”, *Mechanics Industry*, **16**(6), 609. <https://doi.org/10.1051/meca/2015036>.
- Gaitonde, V.N., Karnik, S.R., Figueira, L. and Paulo Davim, J. (2009a), “Machinability investigations in hard turning of AISI D2 cold work tool steel with conventional and wiper ceramic inserts”, *Int. J. Refractory Metals Hard Mater.*, **27**(4), 754-763. <https://doi.org/10.1016/j.ijrmhm.2008.12.007>
- Gaitonde, V.N., Karnik, S.R., Figueira, L. and Davim, J.P. (2009b), “Analysis of machinability during hard turning of cold work tool steel (Type: AISI D2)”, *Mater. Manufact. Processes*, **24**(12), 1373-1382. <https://doi.org/10.1080/10426910902997415>.
- Gaitonde, V.N., Karnik, S.R., Figueira, L. and Davim, J.P. (2010), “Performance comparison of conventional and wiper ceramic inserts in hard turning through artificial neural network modeling”, *Int. J. Adv. Manufact. Technol.*, **52**(1-4), 101-114. <https://doi.org/10.1007/s00170-010-2714-3>.
- Grzesik, W. (2008), Machining of hard materials, In: J. Paulo Davim (ed.), *Machining Fundamentals and Recent Advances*. Springer-Verlag, London.
- Günay, M. and Yücel, E. (2013), “Application of Taguchi method for determining optimum surface roughness in turning of high-alloy white cast iron”, *Measurement*, **46**(2), 913-919. <https://doi.org/10.1016/j.measurement.2012.10.013>.
- Hessainia, Z., Belbah, A., Yallese, M.A., Mabrouki, T. and Rigal, J.F. (2013), “On the prediction of surface roughness in the hard turning based on cutting parameters and tool vibrations”, *Measurement*, **46**(5), 1671-1681. <https://doi.org/10.1016/j.measurement.2012.12.016>.
- Kablouti, O., Boulanouar, L., Azizi, M.A. and Yallese, M.A. (2017), “Effects of coating material and cutting parameters on the surface roughness and cutting forces in dry turning of AISI 52100 steel”, *Struct. Eng. Mech.*, **61**(4), 519-526. <https://doi.org/10.12989/sem.2017.61.4.519>.
- Khamel, S., Ouelaa, N. and Bouacha, K. (2012), “Analysis and prediction of tool wear, surface roughness and cutting forces in hard turning with CBN tool”, *J. Mech. Sci. Technol.*, **26**(11), 3605-3616. <https://doi.org/10.1007/s12206-012-0853-1>.
- Khellaf, A., Aouici, H., Smaiah, S., Boutabba, S., Yallese, M.A. and Elbah, M. (2016), “Comparative assessment of two ceramic cutting tools on surface roughness in hard turning of AISI H11 steel: including 2D and 3D surface topography”, *Int. J. Adv. Manufact. Technol.*, **89**(1-4), 333-354. <https://doi.org/10.1007/s00170-016-9077-3>.
- Kishawy, H.A. and Elbestawi, M.A. (2001), “Tool wear and surface integrity during high-speed turning of hardened steel with polycrystalline cubic boron nitride tools”, *Proceedings of the Institution of Mechanical Engineers, Part B: J. Eng. Manufact.*, **215**(6), 755-767. <https://doi.org/10.1243/0954405011518700>.
- Kumar, P. and Chauhan, S.R. (2015), “Machinability study on finish turning of AISI H13 hot working die tool steel with Cubic Boron Nitride (CBN) cutting tool Inserts using response Surface Methodology (RSM)”, *Arabian J. Sci. Eng.*, **40**(5), 1471-1485. <https://doi.org/10.1007/s13369-015-1606-0>.
- Kumar, R., Sahoo, A.K., Mishra, P.C. and Das, R.K. (2018). “Comparative study on machinability improvement in hard turning using coated and uncoated carbide inserts: part II modeling, multi-response optimization, tool life, and economic aspects”, *Adv. Manufact.*, **6**(2), 155-175. <https://doi.org/10.1007/s40436-018-0214-0>.
- Kumar, S., Singh, D. and Kalsi, N.S. (2016), “Surface quality evaluation of AISI 4340 steel having varying hardness during machining with TiN-coated CBN inserts”, *Proceedings of the Institution of Mechanical Engineers, Part J: Eng. Tribology*, **231**(7), 925-933. <https://doi.org/10.1177/1350650116684243>.
- Laouissi, A., Yallese, M.A., Belbah, A., Belhadi, S. and Haddad, A. (2018), “Investigation, modeling, and optimization of cutting parameters in turning of gray cast iron using coated and uncoated silicon nitride ceramic tools. Based on ANN, RSM, and GA optimization”, *Int. J. Adv. Manufact. Technol.*, **101**(1-4), 523-548. <https://doi.org/10.1007/s00170-018-2931-8>.
- Liu, M., Takagi, J. and Tsukuda, A. (2004), “Effect of tool nose radius and tool wear on residual stress distribution in hard turning of bearing steel”, *J. Mater. Processing Technol.*, **150**(3), 234-241. <https://doi.org/10.1016/j.jmatprotec.2004.02.038>.
- Meddour, I., Yallese, M.A., Khattabi, R., Elbah, M. and Boulanouar, L. (2014), “Investigation and modeling of cutting forces and surface roughness when hard turning of AISI 52100 steel with mixed ceramic tool: cutting conditions optimization”, *Int. J. Adv. Manufact. Technol.*, **77**(5-8), 1387-1399. <https://doi.org/10.1007/s00170-014-6559-z>.
- Meddour, I., Yallese, M.A., Bensouilah, H., Khellaf, A. and Elbah, M. (2018), “Prediction of surface roughness and cutting forces using RSM, ANN, and NSGA-II in finish turning of AISI 4140 hardened steel with mixed ceramic tool”, *Int. J. Adv. Manufact. Technol.*, **97**(5-8), 1931-1949. <https://doi.org/10.1007/s00170-018-2026-6>.
- Mondal, K. and Das, S. (2017), “An investigation on machinability during turning hardened steel in dry condition”, *J. Institution Engineers (India): Series C*, **99**(6), 637-644. <https://doi.org/10.1007/s40032-017-0370-1>.
- Nayak, M. and Sehgal, R. (2015), “Effect of tool material properties and cutting conditions on machinability of AISI D6 steel during hard turning”, *Arabian J. Sci. Eng.*, **40**(4), 1151-1164. <https://doi.org/10.1007/s13369-015-1578-0>
- Nouioua, M., Yallese, M.A., Khattabi, R., Belhadi, S., Bouhalais, M.L. and Girardin, F. (2017), “Investigation of the performance of the MQL, dry, and wet turning by response surface methodology (RSM) and artificial neural network (ANN)”, *Int. J. Adv. Manufact. Technol.*, **93**(5-8), 2485-2504. <https://doi.org/10.1007/s00170-017-0589-2>.
- Panda, A., Sahoo, A.K. and Rout, A.K. (2016), “Investigations on surface quality characteristics with multi-response parametric optimization and correlations”, *Alexandria Eng. J.*, **55**(2), 1625-1633. <https://doi.org/10.1016/j.aej.2016.02.008>.
- Panda, A., Das, S.R. and Dhupal, D. (2017), “Surface roughness analysis for economical feasibility study of coated ceramic tool in hard turning operation”, *Process Integration Optim. Sustainability*, **1**(4), 237-249. <https://doi.org/10.1007/s41660-017-0019-9>.
- Quiza, R., Figueira, L. and Paulo Davim, J. (2007), “Comparing statistical models and artificial neural networks on predicting the tool wear in hard machining D2 AISI steel”, *Int. J. Adv. Manufact. Technol.*, **37**(7-8), 641-648. <https://doi.org/10.1007/s00170-007-0999-7>.
- Sahoo, A.K. and Sahoo, B. (2013), “Performance studies of multilayer hard surface coatings (TiN/TiCN/Al₂O₃/TiN) of indexable carbide inserts in hard machining: Part-II (RSM, grey

- relational and techno economical approach)", *Measurement*, **46**(8), 2868-2884. <https://doi.org/10.1016/j.measurement.2012.09.023>.
- Sharma, V. S., Dhiman, S., Sehgal, R. and Sharma, S.K. (2008), "Estimation of cutting forces and surface roughness for hard turning using neural networks", *J. Intel. Manufact.*, **19**(4), 473-483. <https://doi.org/10.1007/s10845-008-0097-1>.
- Shihab, S.K., Khan, Z.A., Mohammad, A. and Siddiquee, A.N. (2014), "Optimization of surface integrity in dry hard turning using RSM", *Sadhana*, **39**(5), 1035-1053. <https://doi.org/10.1007/s12046-014-0263-4>.
- Shaw, M.C. (2005), *Metal Cutting Principles*, second edition, Oxford University Press, New York.
- Suresh, R., Basavarajappa, S., Gaitonde, V.N. and Samuel, G.L. (2012), "Machinability investigations on hardened AISI 4340 steel using coated carbide insert", *Int. J. Refractory Metals Hard Mater.*, **33**, 75-86. <https://doi.org/10.1016/j.ijrmhm.2012.02.019>.
- Suresh, R., Basavarajappa, S., Gaitonde, V.N., Samuel, G. and Davim, J.P. (2013), "State-of-the-art research in machinability of hardened steels", *Proceedings of the Institution of Mechanical Engineers, Part B: J. Eng. Manufact.*, **227**(2), 191-209. <https://doi.org/10.1177/0954405412464589>.
- Tang, L., Cheng, Z., Huang, J., Gao, C. and Chang, W. (2014), "Empirical models for cutting forces in finish dry hard turning of hardened tool steel at different hardness levels", *Int. J. Adv. Manufact. Technol.*, **76**(1-4), 691-703. <https://doi.org/10.1007/s00170-014-6291-8>.
- Xiao, Z., Liao, X., Long, Z. and Li, M. (2016), "Effect of cutting parameters on surface roughness using orthogonal array in hard turning of AISI 1045 steel with YT5 tool", *Int. J. Adv. Manufact. Technol.*, **93**(1-4), 273-282. <https://doi.org/10.1007/s00170-016-8933-5>.
- Xie, N., Zhou, J. and Zheng, B. (2018), "An energy-based modeling and prediction approach for surface roughness in turning", *Int. J. Adv. Manufact. Technol.*, **96**(5-8), 2293-2306. <https://doi.org/10.1007/s00170-018-1738-y>.
- Zerti, O., Yallese, M.A., Khettabi, R., Chaoui, K. and Mabrouki, T. (2016), "Design optimization for minimum technological parameters when dry turning of AISI D3 steel using Taguchi method", *Int. J. Adv. Manufact. Technol.*, **89**(5-8), 1915-1934. <https://doi.org/10.1007/s00170-016-9162-7>.
- Zerti, A., Yallese, M.A., Meddour, I., Belhadi, S., Haddad, A. and Mabrouki, T. (2018), "Modeling and multi-objective optimization for minimizing surface roughness, cutting force, and power, and maximizing productivity for tempered stainless steel AISI 420 in turning operations", *Int. J. Adv. Manufact. Technol.*, doi:10.1007/s00170-018-2984-8.
- Zhao, T., Zhou, J.M., Bushlya, V. and Ståhl, J.E. (2017), "Effect of cutting edge radius on surface roughness and tool wear in hard turning of AISI 52100 steel", *Int. J. Adv. Manufact. Technol.*, **91**(9-12), 3611-3618. <https://doi.org/10.1007/s00170-017-0065-z>